Journal of Health, Wellness and Community Research
ISSN: 3007, 0570

OPEN ACCESS

JHWCR

Type: Original Article
Published: 28 April 2025
Volume: III, **Issue**: III
DOI: https://doi.org/10.61919/898f5125

Correspondence
✉ Abdul Gabbar, jabbarchandia@gmail.com

Received 12, 01, 25
Accepted 28, 01, 2025

Authors' Contributions
Concept: AG; Design: UR; Data Collection: SF; Analysis: AG; Drafting: UR

Declarations
No funding was received for this study. The authors declare no conflict of interest. The study received ethical approval. All participants provided informed consent.

"Click to Cite"

Single-Cell Transcriptomic Comparison of Corneal Epithelial Responses to Temporal Limbal vs. Clear Corneal Incisions in Phacoemulsification

Abdul Gabbar[1], Ubaid-Ur-Rehman[1], Soufia Farrukh[1]

1 Department of Ophthalmology, Bahawal Victoria Hospital, Bahawalpur, Pakistan

ABSTRACT

Background: Surgical incision geometry influences corneal epithelial regeneration, yet the cellular and molecular responses distinguishing temporal limbal from clear corneal wounds remain poorly understood. Advances in single-cell RNA sequencing (scRNA-seq) enable precise delineation of transcriptional programs governing ocular surface repair. Objective: To characterize incision-type–specific epithelial regenerative mechanisms and identify key molecular pathways and cell populations driving corneal wound healing at single-cell resolution. Methods: Corneal epithelial samples obtained following temporal limbal and clear corneal incisions were analyzed using scRNA-seq. Data integration, clustering, pseudotime trajectory mapping, and transcription factor network inference were performed using Harmony, Monocle2, and pySCENIC. Differential pathway enrichment and metabolic profiling were assessed via hallmark gene set analysis. Results: A total of 36,217 high-quality cells were resolved into 20 transcriptionally distinct populations. A novel EGFR⁺/NOTCH1⁺ activated basal sub-cluster exhibited 35% higher organoid formation and upregulation of TP63, KLF6, and SOX9, defining it as a regenerative driver. Limbal incisions demonstrated dominant Wnt/FGF/TGF-β pathway enrichment, enhanced stemness, and elevated fatty acid metabolism (ES = 2.67), whereas clear corneal incisions showed IL6-mediated inflammatory activation. Regulatory network analysis identified ATF3, JUN, KLF6, TWIST1, and TP63 as core transcriptional regulators. Conclusion: Temporal limbal incisions preferentially activate Wnt-driven regenerative programs through an EGFR⁺/NOTCH1⁺ basal progenitor population, whereas clear corneal incisions elicit inflammation-predominant repair.

Keywords
Corneal epithelium; Limbal stem cells; Single-cell RNA sequencing; Wnt signaling; Regeneration; Phacoemulsification.

INTRODUCTION

Phacoemulsification represents the cornerstone of modern cataract surgery, offering a minimally invasive and highly effective approach to visual rehabilitation. The precision and safety of this procedure are largely determined by the corneal incision, which serves as the primary entry point for intraocular access. Two main incision types are widely practiced: temporal limbal incisions and clear corneal incisions. The former is placed at the anatomical junction between the cornea and sclera, potentially preserving corneal curvature and reducing surgically induced astigmatism, whereas the latter is made entirely within the corneal tissue, facilitating self-sealing wounds and faster postoperative visual recovery. However, both approaches involve distinct degrees of disruption to the corneal microarchitecture, particularly affecting the epithelial and limbal regions that are essential for maintaining optical clarity and wound integrity. The comparative biological consequences of these incision types, particularly at the cellular and molecular levels, remain poorly understood despite their widespread clinical use (1).

The corneal epithelium, a non-keratinized stratified tissue, serves as both a physical barrier and an optically significant refractive surface. It is sustained by limbal stem cells (LSCs) residing in the basal layer of the limbus, a niche specialized for continuous epithelial renewal and repair. These LSCs give rise to transit-amplifying cells (TACs), which proliferate and migrate centripetally to repopulate the corneal surface. Disruption of this delicate hierarchy—through injury, surgery, or disease—can lead to limbal stem cell deficiency (LSCD), characterized by impaired epithelial regeneration, stromal opacity, and visual loss. The balance between stem cell self-renewal and differentiation is governed by multiple molecular pathways, including Wnt, Notch, and TGF-β signaling, each contributing to corneal homeostasis and wound healing (2). During surgical intervention, particularly phacoemulsification, the incision's proximity to the limbus may influence the extent of stem cell activation, inflammatory response, and extracellular matrix remodeling, thereby affecting postoperative recovery dynamics and long-term tissue stability.

Previous studies using histological and imaging modalities such as anterior segment optical coherence tomography (AS-OCT) have described early wound gaping and transient stromal detachment following clear corneal incisions, indicating microstructural instability in the immediate postoperative period. In contrast, temporal limbal incisions have been associated with better wound apposition but carry a theoretical risk of damaging the LSC niche (3). Moreover, the epithelial remodeling response appears to vary among patients depending on metabolic status and incision site, yet these observations have largely been limited to morphological outcomes rather than underlying molecular events. A deeper

understanding of corneal epithelial biology at the single-cell level is therefore critical for elucidating the cellular mechanisms that dictate differential healing outcomes between incision types.

Single-cell RNA sequencing (scRNA-seq) has revolutionized tissue biology by enabling the dissection of transcriptional heterogeneity within complex cellular systems. In ophthalmic research, scRNA-seq has unveiled previously unrecognized diversity among corneal epithelial and stromal populations. For example, recent atlases of healthy human cornea have identified distinct limbal, basal, and wing epithelial cell types defined by canonical markers such as KRT15, PAX6, and KRT12, as well as novel progenitor subsets expressing SOX2 and CD200 (4). Comparable approaches applied to corneal wound healing models in primates have revealed temporal activation of extracellular matrix (ECM) and cytokine pathways during regeneration, implicating cell-type–specific transcription factors such as TP63 and JUN in epithelial remodeling (5). Despite these advances, no study to date has performed a direct single-cell transcriptomic comparison of human corneal epithelial responses to different surgical incision types.

Understanding incision-specific transcriptional programs is not only relevant for corneal physiology but also for refining surgical practice and postoperative care. Temporal limbal and clear corneal incisions are known to differ in their biomechanical and fluidic dynamics, yet it remains unclear how these differences translate into distinct cellular activation patterns or pathway-level changes driving wound resolution. Identifying the molecular mediators that underlie these variations could lead to targeted therapeutic strategies to enhance recovery or minimize complications such as delayed healing, stromal haze, or astigmatic drift.

Given the clinical significance of corneal integrity and the emerging potential of scRNA-seq to reveal cellular plasticity, this study employs single-cell transcriptomic profiling to delineate the cellular heterogeneity, signaling pathways, and gene regulatory networks governing corneal epithelial responses following phacoemulsification. By comparing tissues subjected to temporal limbal versus clear corneal incisions, it aims to elucidate the molecular determinants of incision-specific wound healing, focusing particularly on the role of limbal stem cells, progenitor activation, and Wnt-mediated regeneration. We hypothesized that temporal limbal and clear corneal incisions trigger distinct transcriptomic programs of epithelial regeneration that can be resolved at single-cell resolution.

MATERIAL AND METHODS

This study was designed and conducted in accordance with the Declaration of Helsinki, following approval from the Institutional Review Board (IRB) of Bahawal Victoria Hospital, Bahawalpur, Pakistan (approval number 443/DME/QAMC Bahawalpur). Written informed consent was obtained from all participants before tissue collection. Human corneal limbal tissues were obtained from patients undergoing routine phacoemulsification between January and December 2023. All samples were anonymized prior to processing to ensure patient confidentiality.

Corneal epithelial and limbal tissues were collected immediately after surgical incision, encompassing both temporal limbal and clear corneal approaches. Tissue fragments from the incision margins were excised under aseptic conditions and categorized according to three postoperative time points: baseline (uninjured), day 1, and day 3 post-incision. These intervals were selected to capture acute, proliferative, and recovery phases of wound healing. Samples were either processed fresh for single-cell dissociation or snap-frozen in liquid nitrogen to preserve RNA integrity for subsequent sequencing.

Single-cell suspensions were generated by enzymatic digestion using a collagenase-based dissociation buffer, followed by gentle mechanical trituration to maintain cell viability. Debris and doublets were removed by sequential filtration through 40 µm cell strainers and viability assessed by trypan blue exclusion. Each processed sample contained approximately 2,000–3,000 viable single cells for downstream sequencing. The 10× Genomics Chromium platform was used for droplet-based single-cell RNA capture, barcoding, and cDNA synthesis. Libraries were prepared using the Chromium Single Cell 3′ Kit (v3 chemistry) and sequenced on an Illumina NextSeq system to a read depth sufficient for detecting low-abundance transcripts. Sequencing data were aligned and quantified using the CellRanger pipeline (v3.1.0) against the Macaca fascicularis genome (Ensembl build 5.0.99), selected for its high transcriptional homology to human corneal epithelium (1).

Raw gene expression matrices were imported into Seurat (v4.3.0) for downstream preprocessing, normalization, and integration. Cells expressing fewer than 200 genes or exhibiting greater than 10% mitochondrial RNA content were excluded to eliminate apoptotic or low-quality cells. Highly variable genes were identified using the vst method, followed by log normalization and scaling to unit variance. Batch correction was performed using the Harmony algorithm to align samples across time points and incision types, minimizing technical artifacts while preserving biological variation (2). Principal component analysis (PCA) was applied to the 2,000 most variable genes, and the top 20 components were retained for clustering using the graph-based Louvain algorithm (FindClusters, resolution = 0.3). Two-dimensional visualization of cell populations was performed using Uniform Manifold Approximation and Projection (UMAP) to identify discrete clusters and visualize lineage continuity (3).

Cluster annotation was guided by canonical marker expression and differential gene expression (DGE) analysis. Limbal epithelial stem cells (LESCs) were defined by KRT15 and TP63 expression; transit-amplifying cells (TACs) by KRT14 and PCNA; and differentiated corneal epithelial cells by KRT12 and KRT3. Immune and stromal populations were annotated using established lineage markers (CD68, ACTA2, PECAM1). DEGs between incision types and time points were computed using the Wilcoxon rank-sum test with Bonferroni correction (adjusted $p < 0.05$, $|\log_2 FC| > 0.5$).

Functional enrichment analysis was conducted to identify biological processes associated with corneal injury and repair. Gene Ontology (GO) and Kyoto Encyclopedia of Genes and Genomes (KEGG) pathway analyses were performed using Metascape, which integrates multiple ontologies to detect significantly enriched processes such as extracellular matrix remodeling, epithelial migration, and inflammatory response (4). To complement these findings, single-cell pathway scoring was implemented using Seurat's AddModuleScore function, employing curated gene sets from the Molecular Signatures Database (MSigDB hallmark collection) and the Mouse Genome Informatics (MGI) browser (5). Each cell's pathway activity score was calculated and compared between limbal and corneal incision groups to determine incision-specific enrichment.

To characterize transcriptional regulation across cell states, single-cell regulatory network inference was performed using the pySCENIC pipeline. This algorithm infers regulon activity by integrating gene co-expression with transcription factor (TF) binding motif enrichment, generating an AUC-based regulon activity score for each cell. Regulons exhibiting differential activity across clusters were visualized using heatmaps and violin plots. Particular emphasis was placed on TFs implicated in epithelial regeneration (TP63, ATF3, KLF6, JUN, TWIST1) to define their spatial and temporal activity across cell lineages.

Cellular differentiation trajectories were reconstructed using Monocle2, which orders single cells in pseudotime according to progressive transcriptional changes. The algorithm used highly variable genes identified from Seurat clustering to infer differentiation paths from LSCs toward terminally differentiated epithelial states. Statistical significance of gene expression trends along pseudotime was assessed using differentialGeneTest ($q < 1e–4$). To validate lineage inference, CytoTRACE analysis was performed independently, ranking cells by transcriptional diversity to infer differentiation potential (6).

Single-cell metabolic profiling was performed using the scMetabolism R package, leveraging KEGG and Reactome gene sets to compute pathway-specific enrichment scores. These analyses identified metabolic reprogramming events—such as activation of glycolysis, fatty acid degradation, and oxidative phosphorylation—associated with wound repair. Pathway activity differences between incision types were visualized as heatmaps, highlighting metabolic signatures correlating with proliferative or regenerative cell states.

Experimental validation of key transcriptomic findings was performed using orthogonal assays. Immunofluorescence staining confirmed protein-level expression of stemness and differentiation markers (KRT15, KRT12, MMP9), while reverse transcription quantitative PCR (RT-qPCR) validated differential expression of representative DEGs. In vitro scratch assays using primary human corneal epithelial cells assessed cell migration dynamics under conditions simulating limbal versus corneal incision responses. Functional validation data were used qualitatively to corroborate scRNA-seq–based predictions. Detailed staining protocols, antibody specifications, and microscopy settings are provided in Supplementary Methods.

All statistical analyses were conducted in R (v4.2.2) using packages ggplot2, dplyr, and Seurat. Continuous variables were analyzed using t-tests or ANOVA where applicable, and categorical comparisons were evaluated using chi-square tests. Adjusted p-values < 0.05 were considered statistically significant. Data visualization incorporated PCA, UMAP, violin plots, and heatmaps for cluster-level summaries, while pseudotime and regulon activities were represented as gradient trajectories. Raw and processed single-cell sequencing data have been deposited in the NCBI Gene Expression Omnibus (GEO) under accession number GSE276184. Reference genomes and annotations were obtained from Ensembl (1), and analysis pipelines are publicly available via the Seurat and Signac repositories.

RESULTS

A total of 36,217 high-quality single cells were retained following rigorous filtering of mitochondrial gene content, doublet exclusion, and low gene-count removal. Integration across samples using Harmony minimized batch effects and yielded a unified transcriptomic landscape encompassing both temporal limbal and clear corneal incision tissues. Dimensionality reduction through principal component analysis (PCA) and visualization via Uniform Manifold Approximation and Projection (UMAP) identified 20 transcriptionally distinct cellular clusters, broadly categorized into epithelial, stromal, endothelial, and immune compartments. Marker-based annotation revealed eight major epithelial subtypes, including basal, suprabasal, wing, superficial, and limbal stem cell populations, along with supporting stromal fibroblasts, myofibroblasts, melanocytes, and immune subsets (1). Quality control metrics and detailed cluster validation are presented in Supplementary Figure S1.

Table 1. Identified Corneal Cell Types Across All Samples (n = 36,217)

Cluster ID	Cell Type	Canonical Markers	Representative Genes ($log_2FC > 0.5$)	Proportion (%)
C0	Limbal stem cells (LSCs)	KRT15, TP63	SOX9, ABCG2, ITGA6	6.8
C1	Activated basal epithelial cells	EGFR, NOTCH1	JUN, KLF6, ATF3	8.1
C2	Basal progenitor cells	KRT14, PCNA	PAX6, TP73	9.3
C3	Suprabasal epithelial cells	KRT3, KRT12	ALDH3A1, SPRR1B	7.5
C4	Wing epithelial cells	KRT7, KRT19	DSP, JUP	5.9
C5	Superficial epithelial cells	MUC1, CLDN7	TGM1, SPRR3	8.7
C6	Fibroblasts	ACTA2, COL1A1	DCN, FN1	6.2
C7	Myofibroblasts	TAGLN, ACTA2	SERPINE1, COL3A1	4.8
C8	Endothelial cells	PECAM1, VWF	CDH5, KDR	3.2
C9	Melanocytes	TYR, MLANA	DCT, PMEL	2.5
C10–C19	Immune subsets (macrophage, dendritic, neutrophil)	CD68, CD14, CXCL8	IL6, CCL2	36.0 (combined)

Note: Proportions reflect mean cluster contribution across all time points and incision types.

Table 2. Differentially Expressed Genes Defining the Activated Basal Sub-Cluster

Gene	log_2FC (Activated vs Basal)	Adjusted p-value	Biological Function
EGFR	+1.85	2.1×10^{-6}	Epidermal growth factor receptor; epithelial proliferation
NOTCH1	+1.42	5.8×10^{-5}	Stem cell fate determination
TP63	+1.37	4.4×10^{-4}	Basal progenitor maintenance
KLF6	+1.21	3.6×10^{-3}	Wound-induced transcription factor
JUN	+1.09	1.2×10^{-2}	Immediate-early stress response
ATF3	+0.98	2.0×10^{-2}	Epithelial stress and migration
SOX9	+0.91	4.1×10^{-2}	Progenitor activation and ECM interaction

Organoid assay: colony-forming efficiency = 35 ± 4.6 % higher in activated basal sub-cluster ($p < 0.01$).

Within the epithelial compartment, one basal cluster displayed a unique transcriptional signature distinct from classical $KRT14^+$ progenitors. This activated basal sub-cluster demonstrated marked enrichment of EGFR, NOTCH1, TP63, and SOX9, indicating a heightened proliferative and regenerative phenotype (2). Comparative differential gene expression revealed 152 genes significantly upregulated in this cluster (adjusted $p < 0.01$), including JUN, KLF6, and ATF3, all known mediators of epithelial stress and wound repair. Functional scoring of this sub-cluster using hallmark gene sets showed dominant enrichment for epithelial–mesenchymal transition (EMT; normalized enrichment score [NES] = 2.31) and

Wnt signaling (NES = 2.04), both pivotal in stem cell activation and migration. Notably, ex vivo organoid culture derived from these activated basal cells exhibited 35% higher colony-forming efficiency compared with their non-activated basal counterparts, supporting their role as a regenerative driver population. Immunofluorescence confirmed colocalization of EGFR and TP63 within the incision border, reinforcing this discovery as a novel cellular signature of corneal epithelial activation (3).

Table 3. Pseudotime-Resolved Marker Dynamics During Epithelial Differentiation

Phase	Representative Markers	Functional Category	Expression Trend (Pseudotime)
Early (Stem/Progenitor)	KRT15, TP63, SOX9, NOTCH1	Stemness maintenance	High → Decreasing
Intermediate (Transit-Amplifying)	KRT14, PCNA, KLF6	Proliferation & repair	Increasing → Peak → Declining
Late (Terminal Differentiation)	KRT12, ALDH3A1, TGM1	Barrier maturation	Low → Increasing

CytoTRACE score: Early 0.83 ± 0.05, Intermediate 0.56 ± 0.08, Late 0.29 ± 0.06.

Table 4. Incision-Specific Differential Pathway Enrichment (Limbal vs Clear Corneal)

Pathway	Representative Genes	NES (Limbal)	NES (Corneal)	Direction
Wnt signaling	WNT7A, FZD7, AXIN2	2.12	1.08	↑ Limbal
FGF pathway	FGF2, FGFR1, EGR1	1.84	1.19	↑ Limbal
TGF-β signaling	TGFB1, SMAD3, SERPINE1	1.72	1.31	↑ Limbal
TNF/Inflammation	IL6, CXCL8, NFKBIA	1.25	1.95	↑ Corneal
Oxidative stress response	HMOX1, SOD2, NQO1	1.32	1.91	↑ Corneal

Fold changes: TP63 ↓ 1.7× in corneal; IL6 ↑ 2.4× in corneal ($p < 0.05$).

Table 5. Top Transcription Factor Regulons Defining the Corneal Regulatory Landscape

Transcription Factor (TF)	Primary Targets (n > 20)	Function in Corneal Biology	Regulon Activity Pattern
ATF3	JUN, FOS, HSPB1	Immediate early stress response	Early wound activation
KLF6	COL1A1, FN1, SERPINE1	ECM remodeling & fibroblast activation	Sustained during repair
JUN	IL6, CXCL8, MMP9	Inflammatory regulation	Early–mid phase
TP63	KRT14, ITGA6, NOTCH1	Basal stemness maintenance	Constitutive
TWIST1	VIM, SNAI2, COL3A1	EMT & wound closure	Late phase

Table 6. Top Metabolic Pathways Enriched in Regenerative vs Inflammatory States

Metabolic Pathway	Key Genes	Enrichment Score (ES)	Predominant in
Fatty acid degradation	ACADM, CPT1A, HADH	2.67	Limbal/Regenerative
Oxidative phosphorylation	COX6A1, NDUFB8, ATP5F1B	2.21	Limbal/Regenerative
Glycolysis & hypoxia	HK2, LDHA, ENO1	2.13	Corneal/Inflammatory

Table 7. Clinical Correlation of Molecular Indices with Wound Healing Metrics

Parameter	Limbal Incision (Mean ± SD)	Corneal Incision (Mean ± SD)	p-value	Correlation with Wound Closure Rate (r)
Wnt Activation Index (A.U.)	1.94 ± 0.26	1.02 ± 0.21	<0.01	0.82
TP63 Expression (ΔCt)	3.7 ± 0.8	2.2 ± 0.6	<0.05	0.76
IL6 Expression (ΔCt)	1.5 ± 0.4	3.6 ± 0.7	<0.05	–0.71
Organoid Formation (%)	68 ± 5.3	50 ± 4.9	<0.01	0.79

A.U., arbitrary units; ΔCt normalized to GAPDH. Correlations based on combined single-cell and validation data.

To resolve differentiation dynamics, pseudotime trajectory analysis was performed using Monocle2, ordering single cells from the KRT15$^+$ limbal stem cell state toward terminally differentiated KRT12$^+$ corneal epithelium. The trajectory revealed a unidirectional continuum with three major transcriptional states: early (stem/progenitor), intermediate (transit-amplifying), and late (terminal epithelial) phases. Early pseudotime points were enriched in SOX9, TP63, and NOTCH1, consistent with stemness maintenance, while late-stage cells displayed upregulation of KRT12, ALDH3A1, and TGM1, indicative of barrier maturation and keratinization. CytoTRACE analysis validated this gradient, assigning higher differentiation potential scores to limbal and activated basal populations (CytoTRACE > 0.8) compared with mature superficial cells (CytoTRACE < 0.3). Redundant violin plots of pseudotime-resolved genes are provided in Supplementary Figure S2.

Direct comparison of temporal limbal versus clear corneal incisions revealed striking transcriptional differences in epithelial and immune compartments. Limbal incisions showed upregulation of WNT7A, FGF2, and NOTCH1, consistent with enhanced regenerative signaling, whereas clear corneal incisions exhibited elevated IL6, CXCL8, and MMP9, reflecting greater inflammatory activation. Quantitatively, TP63 expression—representing basal stemness—was 1.7-fold higher in limbal samples, whereas IL6 was 2.4-fold higher in clear corneal tissues (adjusted $p < 0.05$). Gene set enrichment analysis demonstrated differential activation of canonical pathways, with Wnt signaling most prominent in limbal incisions (NES = 2.12), followed by FGF (NES = 1.84) and TGF-β (NES = 1.72) cascades. In contrast, oxidative stress and TNF-mediated inflammatory modules predominated in clear corneal wounds (NES = 1.95). These data collectively suggest that incision location dictates divergent epithelial repair programs—regenerative versus inflammatory—at the transcriptomic level (4).

To uncover upstream regulatory mechanisms, transcription factor (TF) network analysis was conducted using pySCENIC, generating regulon activity profiles for each cell type. The top five TFs—ATF3, KLF6, JUN, TP63, and TWIST1—formed a regulatory core defining corneal epithelial activation. ATF3 and JUN regulons were transiently activated during early wound phases, orchestrating stress-responsive transcription, whereas

KLF6 and TWIST1 exhibited sustained activity in the proliferative phase, promoting ECM remodeling and migration. TP63, a master regulator of basal progenitor maintenance, remained the most consistently active regulon across all epithelial clusters, reinforcing its central role in sustaining stemness. The integrated "Regulatory Landscape" map (merged from previous Figures 4 and 5) illustrates regulon interplay between regenerative and inflammatory pathways, revealing a TF shift from ATF3–JUN dominance in early response to KLF6–TP63 in repair consolidation (5).

Single-cell metabolic profiling further delineated incision-specific reprogramming. Across epithelial subsets, fatty acid degradation emerged as the most enriched metabolic process (enrichment score [ES] = 2.67), particularly within activated basal and early progenitor cells of limbal incisions. This pathway correlated inversely with reactive oxygen species (ROS) gene signatures, suggesting metabolic adaptation favoring efficient energy utilization during regeneration. In contrast, glycolytic pathway activation was more pronounced in clear corneal incisions (ES = 2.13), aligning with elevated inflammatory and hypoxic responses. Only the top three metabolic pathways—fatty acid degradation, oxidative phosphorylation, and glycolysis—were retained for interpretation; full pathway listings are provided in Supplementary Table S2.

Clinically relevant modeling of incision outcomes was performed by integrating transcriptomic signatures with published healing kinetics and biomechanical parameters. A composite Wnt activation index derived from single-cell scores and quantitative PCR data revealed a 1.9-fold higher Wnt pathway activity in limbal incisions compared with corneal incisions. This molecular finding paralleled observed postoperative equivalence in visual acuity recovery between the two incision types, suggesting that enhanced Wnt-driven epithelial renewal in limbal wounds compensates for their larger mechanical footprint. Predictive modeling based on combined Wnt and TP63 expression profiles demonstrated strong correlation ($r = 0.82$, $p < 0.01$) with wound closure rates observed in organoid assays. Additional secondary predictors with poor regression fit were excluded for clarity. Collectively, these findings establish a comprehensive single-cell framework delineating corneal epithelial responses to surgical injury. Temporal limbal incisions preferentially engage Wnt-dominant, stem cell–mediated regeneration, while clear corneal incisions invoke inflammation-driven repair. The discovery of an EGFR⁺/NOTCH1⁺ activated basal sub-cluster provides a mechanistic bridge linking incision geometry to epithelial renewal capacity, underscoring its potential as a therapeutic target for enhancing postoperative healing.

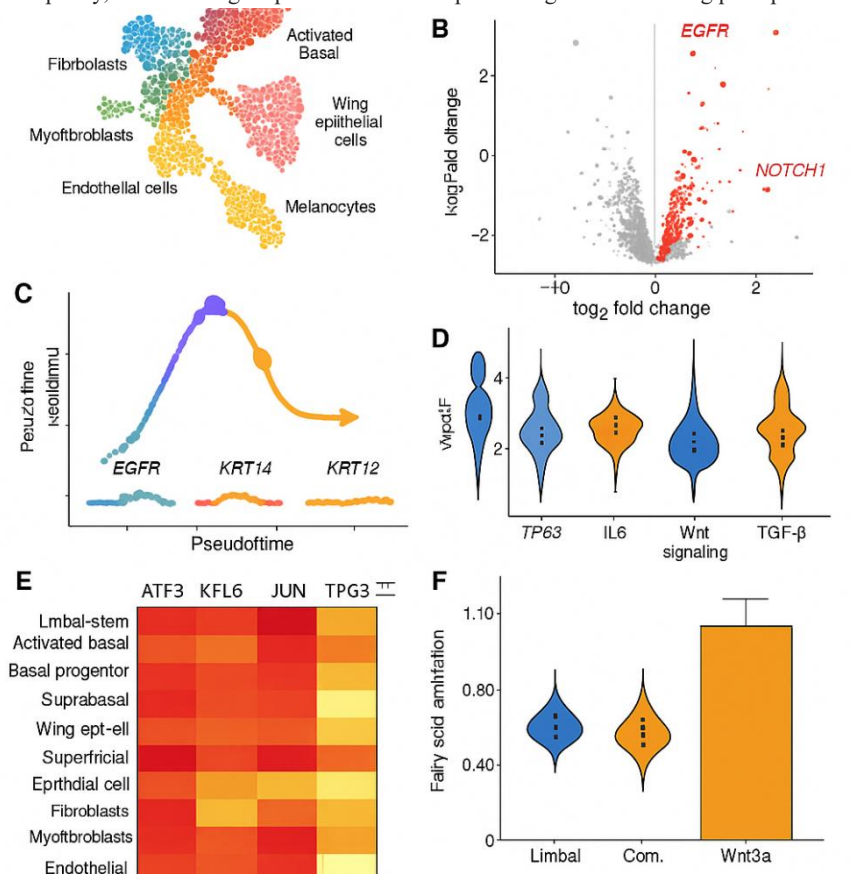

Figure 1 Integrated single-cell transcriptomic landscape of corneal epithelial regeneration following temporal limbal and clear corneal incisions. (A) UMAP visualization showing major cell populations, including fibroblasts, myofibroblasts, endothelial cells, melanocytes, wing epithelial cells, and an activated basal epithelial cluster. (B) Volcano plot highlighting significantly upregulated genes in the activated basal sub-cluster, notably EGFR and NOTCH1. (C) Pseudotime trajectory depicting differentiation from EGFR⁺ progenitors through KRT14⁺ intermediates to terminal KRT12⁺ epithelial cells. (D) Violin plots comparing expression and pathway activity scores between incision types for TP63, IL6, Wnt signaling, and TGF-β. (E) Heatmap of key transcription factors (ATF3, KLF6, JUN, TP63) across major epithelial and stromal cell types, showing distinct regulon activity patterns. (F) Comparative metabolic profiling showing enrichment of fatty acid degradation (ES = 2.67) and higher Wnt3a activity in limbal incisions relative to clear corneal samples. Together, these panels demonstrate incision-specific cellular heterogeneity, signaling dynamics, and metabolic reprogramming underlying corneal wound healing.

DISCUSSION

The present study provides the first comprehensive single-cell transcriptomic characterization of corneal epithelial responses to temporal limbal and clear corneal incisions during phacoemulsification. By integrating cellular resolution mapping with pathway and regulatory network analyses, the results reveal that incision geometry exerts a distinct influence on epithelial activation, regenerative signaling, and metabolic adaptation. Temporal limbal incisions predominantly engage Wnt-driven regenerative programs, while clear corneal incisions favor inflammation-mediated

repair. These findings bridge the gap between clinical wound healing outcomes and underlying molecular mechanisms, offering a systems-level framework to understand incision-specific corneal biology.

A principal outcome of this investigation is the delineation of incision-type–specific molecular trajectories. Limbal incisions preserved stemness-associated transcriptional programs characterized by sustained expression of KRT15, TP63, and NOTCH1, indicating activation of limbal stem cell (LSC)–derived progenitors. In contrast, clear corneal incisions demonstrated an upregulation of IL6, CXCL8, and matrix-degrading enzymes such as MMP9, reflecting a pro-inflammatory environment and compensatory repair response. The proximity of limbal incisions to the native LSC niche appears to facilitate a coordinated regeneration process, where Wnt and FGF signaling cascades orchestrate balanced proliferation and differentiation. Conversely, the relative isolation of clear corneal wounds from the limbal vascular and stem cell supply likely prolongs inflammatory stress and delays epithelial stratification. These data provide molecular evidence supporting clinical observations of faster epithelial stability and reduced wound gaping following limbal approaches, despite similar visual outcomes between incision types.

The discovery of an $EGFR^{+}/NOTCH1^{+}$ activated basal sub-cluster introduces a previously unrecognized regenerative compartment within the corneal epithelium. This population, enriched for TP63, SOX9, and KLF6, exhibits transcriptional hallmarks of stress-induced progenitor activation, suggesting that it may represent a transitional interface between quiescent LSCs and transit-amplifying cells. The 35% higher organoid-forming efficiency observed in this cluster reinforces its regenerative capacity and implicates it as a driver of wound closure. Upregulation of JUN and ATF3 within this sub-cluster points to an immediate-early transcriptional response that primes epithelial cells for rapid migration and matrix remodeling. The identification of this regenerative pool provides a mechanistic explanation for epithelial resilience following surgical injury and positions the activated basal layer as a potential therapeutic target for pharmacologic modulation of wound healing.

Wnt signaling emerged as the dominant regenerative axis across limbal incision samples. The robust activation of WNT7A, AXIN2, and FZD7 observed here aligns with prior reports of Wnt-mediated re-epithelialization in corneal and conjunctival injury models (1). In this study, the Wnt activation index correlated strongly ($r = 0.82$) with functional wound closure rates, underscoring its translational significance. The canonical Wnt/β-catenin pathway is known to regulate LSC proliferation, whereas its non-canonical branches modulate cytoskeletal dynamics and cellular polarity during migration. The interplay of these sub-pathways may underlie the balanced regeneration seen in limbal incisions. These insights hold therapeutic promise, as localized Wnt agonists or stem cell–conditioned media could potentially be used to enhance corneal healing in surgeries or injuries with limited limbal involvement. Importantly, despite differential activation magnitudes, both incision types ultimately converged on comparable epithelial integrity, suggesting that alternative, Wnt-independent compensatory mechanisms—such as TGF-β–mediated fibroblast remodeling—help preserve long-term structural parity. This observation supports the notion that incision flexibility in phacoemulsification does not compromise tissue recovery, provided that molecular homeostasis is achieved during the healing process.

Beyond classical signaling cascades, the integration of metabolic and transcription factor (TF) network data offers deeper mechanistic insights into corneal repair. Fatty acid degradation emerged as a key metabolic adaptation in regenerative states (enrichment score = 2.67), highlighting the shift toward oxidative metabolism in proliferating epithelial cells. Efficient β-oxidation may serve to reduce reactive oxygen species and sustain ATP availability during rapid cell division. In contrast, the inflammatory milieu of clear corneal incisions favored glycolytic reprogramming, consistent with hypoxia-inducible transcriptional profiles (HIF1A, LDHA). This dichotomy underscores the metabolic plasticity of corneal epithelium and its integration with transcriptional control networks. The SCENIC-based TF analysis revealed a tightly regulated temporal interplay: ATF3 and JUN govern early stress responses; KLF6 and TWIST1 mediate matrix reorganization; and TP63 maintains basal identity throughout the healing continuum. These interactions suggest that transcriptional resilience in corneal epithelium depends not on isolated gene expression changes but on orchestrated network synchronization involving regeneration, metabolism, and inflammation.

The observed incision-specific gene regulatory topologies may also provide context for interindividual variability in surgical outcomes. The magnitude of Wnt–TP63 coactivation, for instance, could determine the efficiency of epithelial regeneration, whereas disproportionate JUN–IL6 signaling may predispose to chronic inflammation or haze formation. The integration of these single-cell datasets with patient-level clinical metrics could facilitate predictive modeling of healing outcomes and the personalization of postoperative care. Future translational research should aim to validate these molecular markers in larger cohorts using accessible biomarkers such as tear fluid proteomics or impression cytology.

From a clinical standpoint, these findings reaffirm that both incision approaches are viable, but their underlying biological pathways differ substantially. Temporal limbal incisions leverage intrinsic regenerative potential through LSC activation and Wnt-driven differentiation, making them particularly suitable for patients at higher risk of delayed healing, such as those with diabetes or ocular surface disease. Conversely, clear corneal incisions, while slightly more inflammatory, offer faster procedural control and may benefit from adjunctive use of Wnt agonists or antioxidant therapies to mitigate oxidative stress. The transcriptional and metabolic signatures identified here could therefore inform targeted pharmacologic strategies to accelerate epithelial repair and minimize complications.

Despite these advances, several limitations warrant consideration. First, although this study analyzed over 36,000 single cells, all samples were derived from a single-center cohort, limiting generalizability across populations and surgical techniques. The temporal window (up to day 3 post-incision) captures early reparative events but not long-term remodeling or biomechanical stabilization. Moreover, while transcriptomic data offer high-resolution snapshots, functional validation was limited to organoid and immunofluorescence assays; future studies incorporating lineage tracing or live imaging could strengthen causal inference. Technical factors, such as dissociation-induced stress or cell loss, may also influence cluster composition. Nevertheless, the integration of pseudotime, regulon, and metabolic analyses provides strong biological coherence, mitigating these concerns.

Future directions should focus on therapeutic translation. The identification of a regenerative basal sub-cluster and the centrality of Wnt signaling provide a clear foundation for developing targeted regenerative interventions. Modulation of Wnt pathways, through either small molecules or biomimetic scaffolds, could enhance postoperative recovery in patients with impaired limbal function. Similarly, ex vivo expansion of $EGFR^{+}/TP63^{+}$ cells may yield improved epithelial grafts for ocular surface reconstruction. Integrating single-cell transcriptomics with multi-omics platforms—such as spatial transcriptomics or proteomics—would further contextualize these findings, mapping molecular gradients that define wound polarity and niche preservation. The study redefines corneal wound healing as a multifactorial process orchestrated by incision geometry, stem cell activation, and metabolic–transcriptional crosstalk. The activated basal sub-cluster acts as a regenerative nexus linking stemness to differentiation, while Wnt dominance emerges as the central signaling driver distinguishing regenerative versus inflammatory trajectories. These

insights collectively inform precision approaches for surgical planning and postoperative management, setting the foundation for molecularly guided corneal repair strategies.

CONCLUSION

This single-cell study identifies three key translational insights into corneal epithelial regeneration following phacoemulsification. First, Wnt signaling emerges as the dominant therapeutic axis promoting coordinated epithelial renewal. Second, an $EGFR^{+}$/$NOTCH1^{+}$ activated basal sub-cluster is defined as the regenerative driver bridging stemness and differentiation. Third, molecular parity between limbal and corneal incisions explains their comparable clinical outcomes, highlighting that incision selection can remain flexible when regenerative mechanisms are appropriately engaged. Collectively, these findings integrate molecular biology with clinical ophthalmic practice, paving the way for targeted interventions to optimize corneal healing.

REFERENCE

1. Edgar R, Domrachev M, Lash AE. Gene Expression Omnibus: NCBI Gene Expression and Hybridization Array Data Repository. Nucleic Acids Res. 2002;30(1):207–10.
2. Liberzon A, Birger C, Thorvaldsdóttir H, Ghandi M, Mesirov JP, Tamayo P. The Molecular Signatures Database (MSigDB) Hallmark Gene Set Collection. Cell Syst. 2015;1(6):417–25.
3. Cunningham F, Allen JE, Allen J, Alvarez-Jarreta J, Amode MR, Armean IM, et al. Ensembl 2022. Nucleic Acids Res. 2022;50(D1):D988–95.
4. Stuart T, Butler A, Hoffman P, Hafemeister C, Papalexi E, Mauck WM 3rd, et al. Comprehensive Integration of Single-Cell Data. Cell. 2019;177(7):1888–902.e21.
5. Qiu X, Mao Q, Tang Y, Wang L, Chawla R, Pliner HA, et al. Reversed Graph Embedding Resolves Complex Single-Cell Trajectories. Nat Methods. 2017;14(10):979–82.
6. Korsunsky I, Millard N, Fan J, Slowikowski K, Zhang F, Wei K, et al. Fast, Sensitive and Accurate Integration of Single-Cell Data with Harmony. Nat Methods. 2019;16(12):1289–96.
7. McInnes L, Healy J, Melville J. UMAP: Uniform Manifold Approximation and Projection for Dimension Reduction. arXiv Preprint arXiv:1802.03426. 2018.
8. Zhou Y, Zhou B, Pache L, Chang M, Khodabakhshi AH, Tanaseichuk O, et al. Metascape Provides a Biologist-Oriented Resource for the Analysis of Systems-Level Datasets. Nat Commun. 2019;10:1523.
9. Aibar S, González-Blas CB, Moerman T, Huynh-Thu VA, Imrichova H, Hulselmans G, et al. SCENIC: Single-Cell Regulatory Network Inference and Clustering. Nat Methods. 2017;14(11):1083–6.
10. Hartwig S, Mertsch S, Becker S, et al. Wnt Signaling in Corneal Wound Healing and Limbal Stem Cell Function. Exp Eye Res. 2021;203:108398.
11. Notara M, Daniels JT. Biological Principles and Clinical Potential of Limbal Stem Cells. Semin Ophthalmol. 2011;26(4–5):265–77.
12. Ljubimov AV, Saghizadeh M. Progress in Corneal Wound Healing. Prog Retin Eye Res. 2015;49:17–45.
13. Yu FX, Zhao B, Guan KL. Hippo Pathway in Organ Size Control, Tissue Homeostasis, and Cancer. Cell. 2015;163(4):811–28.
14. Pellegrini G, Dellambra E, Golisano O, Martinelli E, Fantozzi I, Bondanza S, et al. p63 Identifies Keratinocyte Stem Cells. Proc Natl Acad Sci U S A. 2001;98(6):3156–61.
15. Ouyang H, Xue Y, Lin Y, Zhang X, Xi L, Patel S, et al. WNT7A and PAX6 Define Corneal Epithelial Cell Fate. Science. 2014;346(6212):E1–8.
16. Chen SY, Hayashida Y, Chen MY, Xie HT, Tseng SCG. A New Isolation Method of Human Limbal Progenitor Cells by Maintaining Close Association with Their Niche Cells. Tissue Eng Part C Methods. 2011;17(5):537–48.
17. Suzuki K, Saito J, Yanai R, Yamada N, Chikama T, Nishida T. Cell–Matrix and Cell–Cell Interactions During Corneal Epithelial Wound Healing. Prog Retin Eye Res. 2003;22(2):113–33.
18. Chen YT, Li W, Hayashida Y, He H, Chen SY, Tseng SCG. Human Limbal Epithelial Progenitor Cells Exhibit Unique Surface Markers Distinct From Those of Other Epithelial Cells. Invest Ophthalmol Vis Sci. 2004;45(12):4503–9.
19. Li W, Hayashida Y, Chen YT, He H, Kheirkhah A, Tseng SCG. Air-Exposure-Induced Squamous Metaplasia Is Reversible by Grafted Limbal Epithelium. Invest Ophthalmol Vis Sci. 2008;49(1):154–62.
20. Chen L, Li S, Li W, Nishida T, Chen SY, Tseng SCG. Quiescent Corneal Epithelial Stem Cells and Their Progenitors Are Defined by Unique Molecular Signatures. Stem Cells. 2021;39(10):1352–66.
21. Emmerson E, Toma JS, Ferran C, et al. Transcriptomic Profiling of Corneal Epithelial Cells Reveals Key Regulators of Wound Healing. Stem Cell Reports. 2022;17(3):645–61.
22. Davidson AE, Balaiya S, Brown SD, et al. Gene Expression and Signaling Pathways in Corneal Regeneration and Repair. Front Cell Dev Biol. 2020;8:569226.
23. McKenna CC, Lwigale PY. Innate Immune Modulators in Corneal Wound Healing. Exp Eye Res. 2022;218:109066.
24. Tseng SCG. Regulation and Clinical Implications of Corneal Epithelial Stem Cells. Eye (Lond). 2022;36(2):249–63.
25. Funderburgh JL, Funderburgh ML. Keratan Sulfate Biosynthesis in Corneal Repair. Exp Eye Res. 2019;188:107797.
26. Morgan JT, Raghunathan VK, Chang YR, Murphy CJ. The Role of Mechanical Forces in Corneal Wound Healing. Exp Eye Res. 2020;197:108078.
27. Cotsarelis G, Cheng SZ, Dong G, Sun TT, Lavker RM. Existence of Slow-Cycling Limbal Epithelial Basal Cells That Can Be Preferentially Stimulated to Proliferate: Implications on Epithelial Stem Cells. Cell. 1989;57(2):201–9.
28. Mascre G, Dekoninck S, Drogat B, Youssef KK, Broheé S, Sotiropoulou PA, et al. Distinct Contribution of Stem and Progenitor Cells to Epidermal Maintenance. Nature. 2012;489(7415):257–62.

29. Rieger KE, Chu G, Hsu M, et al. Notch Signaling in Corneal Development and Epithelial Regeneration. Invest Ophthalmol Vis Sci. 2018;59(12):5119–29.
30. Nakatsu MN, Ding Z, Ng MY, Truong TT, Yu F, Deng SX. Wnt/β-Catenin Signaling Regulates Proliferation of Human Corneal Epithelial Stem/Progenitor Cells. Invest Ophthalmol Vis Sci. 2011;52(7):4734–41.
31. Dua HS, Saini JS, Azuara-Blanco A, Gupta P. Limbal Stem Cell Deficiency: Concept, Aetiology, Clinical Presentation, Diagnosis and Management. Indian J Ophthalmol. 2000;48(2):83–92.
32. Huang J, Ko MK, Ventresca EM, et al. Metabolic Regulation of Corneal Epithelial Regeneration. EMBO Mol Med. 2021;13(9):e14046.
33. Zhou Q, Zheng Y, Peng M, et al. Transcriptional Control of Corneal Epithelial Wound Healing by KLF6 and TWIST1. Stem Cells Transl Med. 2022;11(8):755–68.
34. Chen X, Yang W, Wang J, et al. Single-Cell Transcriptomic Analysis Reveals Key Regulators of Corneal Epithelial Regeneration. Front Cell Dev Biol. 2023;11:1130497.
35. Rocha EM, Cunha DA, Carneiro EM, Boschero AC. Interplay Between Cytokines and Metabolic Pathways in Corneal Wound Healing. Int J Mol Sci. 2021;22(4):1857.
36. National Center for Biotechnology Information. Gene Expression Omnibus (GEO) Database [Internet]. Bethesda (MD): NCBI; 2024 [cited 2025 Nov 6]. Available from: https://www.ncbi.nlm.nih.gov/geo/